

Some Recent Results in Au+Au collisions at AGS

Ziping Chen
Dept. of Physics
Brookhaven National Lab.
Upton NY, 11973

Many interesting results have been obtained for Au+Au reactions at AGS. The basic information about the reaction dynamics comes from the hadronic distribution, and this article reviews the recent progress of these distributions in details. The proton rapidity distribution shows significantly increased stopping compared to lighter systems, implying the formation of a state of high baryon density. Unlike reactions at this energy induced by lighter heavy ions, at low $m_t - m_0$ the proton invariant spectra deviate from a single exponential shape and become flat, while pion spectra are found to rise in this region, with the π^- spectra rising faster than the π^+ spectra. The inverse slope parameter increases faster for particles of larger mass as the number of participant in the reaction increases, an indication of increased effect of radial expansion in central collision. Anti-proton yields have been measured recently, and unfortunately a comparison among current results from different experiments indicates discrepancy.

MASTER

DISTRIBUTION OF THIS DOCUMENT IS UNLIMITED



I. INTRODUCTION

At AGS energies collisions of heavy ions provide a unique opportunity for studying nuclear matter far from its normal density. This condition is made possible because of the large degree of stopping of the incident nucleons. Hadron spectra which result from collisions of silicon beams with targets ranging from aluminum to gold indicate that the projectile deposits essentially all its incident energies in target larger than copper [1]. It is anticipated that an interaction region of larger volume, longer lifetime, and higher maximum density could be achieved by the collision of two truly heavy ions such as gold. With the installation of the Booster, the Brookhaven Tandem-AGS complex is capable of accelerating Au ions with energies up to 11.6 A-GeV/c. Some of the phenomena which have been considered to be associated with such large degree of stopping include effects of the compression and heating of nuclear matter, the production of a state of very high nucleonic density, and the achievement of thermal and chemical equilibrium. Most speculatively, it has been conjectured that a sufficiently high baryonic density can be attained to effect a phase change from the initial hadronic matter to a quark-gluon plasma. The basic information about the dynamics of these reactions comes from measurements of the transverse momentum and rapidity distributions of hadron spectra. In particular, the proton distributions allow the determination of the nucleonic stopping in the reactions. The article does not intend to cover all the topics studied by the heavy ion experiments at AGS, but rather concentrate on hadronic spectra of various particle species.

II. RESULTS AND DISCUSSION

Figure 1 shows the measured invariant spectra of E866 for protons at different rapidity intervals. On the horizontal axis m_t is the so-called transverse mass defined as $m_t = \sqrt{p_t^2 + m_0^2}$, where p_t is the transverse momentum and m_0 is the rest mass of the identified particle. On the vertical scale is the invariant cross-section divided by the trigger cross section σ_{trig} where $\sigma_{trig} = 350$ mb corresponds to 6% of the total interaction cross section. The solid points are the measurement from the Forward Spectrometer while the open ones are from the large aperture spectrometer. Beam rapidity for Au ions at 11.6 A-GeV/c is 3.2. Since projectile and target are identical, the cross-section is therefore symmetric around the mid-rapidity, $y_{nn} = 1.6$. This symmetry is used to fold spectra of same δy together, where δy is the distance of the measured rapidity y from the central rapidity $\delta y = |y - y_{nn}|$. This experiment covers a rapidity range up to $\delta y = 1.05$ with the projectile (or target) rapidity corresponds to $\delta y = 1.6$. The curves in the figure are the fits to the spectra with a two exponential function.

Proton spectra are also measured in E877, but in a different kinematic region close to the beam rapidity, as indicated in Figure 2 [2]. The vertical axis is slightly different from Figure 1, and the spectra are once again displaced by a factor of 10. The inverse slope of the spectra decreases as the rapidity increases. Around the beam rapidity, $y_b = 3.2$, another component appears in the spectra at low m_t which is even steeper in slope. These are the nucleons which do not go through any violent collision.

To inspect the shapes of the particle spectra in more detail, the measured particle distributions for π^+ , π^- , and protons are displayed in Figure 3 as a function of $m_t - m_0$ for the central rapidity interval of $0 < \delta y < 0.2$, where the proton spectrum has been multiplied by 0.5 for clarity. Clearly, the proton spectrum is much flatter compared with those for pions, and it tends to bend down at low $m_t - m_0$. Hence unlike the proton spectra measured in reactions induced by lighter projectiles at similar incident energy per nucleon, namely p+A [3] and Si+A [4,5], the proton spectrum here cannot be described satisfactorily by a single exponential fit. The spectrum for π^- is also impossible to describe satisfactorily with a single exponential, since it shows a strong rise at low $m_t - m_0$. The rise at low $m_t - m_0$ for π^+ is much less. The rise of both pion spectra at the low $m_t - m_0$ can be explained, in part, by the decay of resonances such as Δ 's which tend to produce relatively low momentum pions [6]. Spectra for π^- increase faster than those for π^+ in this region, and there are several reasons for this. The weak decay of the lambda produces relatively low momentum π^- , and some of these π^- survive the target position cut and show up in the low m_t region. Also the production of low momentum pions through Δ 's prefers π^- [7] because there are more neutrons than protons in the projectile/target. However, a major contributor to the difference between the π^- and π^+ spectra may well be

DISCLAIMER

**Portions of this document may be illegible
in electronic image products. Images are
produced from the best available original
document.**

DISCLAIMER

This report was prepared as an account of work sponsored by an agency of the United States Government. Neither the United States Government nor any agency thereof, nor any of their employees, makes any warranty, express or implied, or assumes any legal liability or responsibility for the accuracy, completeness, or usefulness of any information, apparatus, product, or process disclosed, or represents that its use would not infringe privately owned rights. Reference herein to any specific commercial product, process, or service by trade name, trademark, manufacturer, or otherwise does not necessarily constitute or imply its endorsement, recommendation, or favoring by the United States Government or any agency thereof. The views and opinions of authors expressed herein do not necessarily state or reflect those of the United States Government or any agency thereof.

their Coulomb interaction with the rest of the co-moving media [8-10] which in average is positively charged. In the insert, the ratio (π^-/π^+) is plotted with a larger rapidity bin, $0 < \delta y < 0.4$, and the normalization is absolute. At high $m_t - m_0$, the ratio approaches one.

Figure 4 shows the same ratio, π^-/π^+ , at the same rapidity in reactions of different centralities. The spectra are scaled up by a factor of 2 successively, and the horizontal lines are the corresponding positions for the ratio 1. In peripheral reactions, the ratio is flat over the entire m_t range and its value above one. This is consistent with the fact that there are more neutrons than protons in the colliding nuclei. For comparison, the ratio not only rises at low m_t but also falls down to unity at high m_t in central collisions. This is what would happen if the positive pions were pushed away and the negative pions were pulled in, for example by Coulomb interaction. So the centrality dependency of the π^-/π^+ ratio provides support to the picture of pions interacting with the co-moving medium of positive charge in average.

The rapidity dependence of this ratio is also studied by E877, as illustrated in Figure 5 [2]. In this figure, π^-/π^+ is plotted for events of the 4% most central reactions as a function of $m_t - m_0$. The rapidity interval are indicated in each panel. For rapidity interval smaller than the beam rapidity similar trend of the ratio is observed as in E866, and the m_t dependence of the ratio is weakened around the beam rapidity. Beyond beam rapidity, the ratio is almost flat. Again, this is consistent with the picture discussed above, since most of the protons which provide the positive charge in the medium reside around the central rapidity as discussed later.

By integrating the parameterization of the spectra over $m_t - m_0$ in each rapidity bin, one can obtain the distribution of particle yield over rapidity, dn/dy . The left panel of Figure 6 shows the dn/dy distribution for pions, kaons, and protons. The error bars shown in the figure are statistical only. The spectrum for protons is scaled up by a factor of 10. As indicated in the figure, the centrality for the different particle species is slightly different: 7% most central events for protons and pions, and 10% most central events for kaons and anti-protons. The overall shapes of the rapidity distribution for all the particles are similar. There are more π^- than π^+ , as is expected from the low m_t rise of the π^- . Roughly there are a factor of 5 more K^+ than K^- . With a limited statistics for anti-protons, its yield is presented within a big bin. On the right hand side of the figure, the mean transverse momentum is plotted for the various particles. The mean p_t for protons is very high and peaked around the central rapidity. Anti-protons have similar, though slightly lower, value as protons. The mean p_t for π^+ is a little higher than that for π^- . Both kaons have similar p_t , and their values are in between of those for protons and pions.

Figure 7 shows the rapidity distributions for protons and pions from the p+p collisions to the central Au+Au reactions. The horizontal axis is the rapidity normalized to the beam rapidity, and the vertical axis is the yield, dn/dy . For protons, the rapidity distribution for p+p has two peaks around the projectile and target rapidities respectively, indicating that most of the protons keep traveling at almost the same rapidity before and after the collision, little stopping by the reaction. The situation does not change significantly for peripheral collisions of Al+Si, an almost symmetric system, and in central Al+Si there is significant shifting in rapidity away from the projectile and the target, but a hole in the central rapidity still exists. Only in the central Au+Au reactions, due to the large size of the gold ions, protons pile up at mid-rapidity, with the hole in the middle filled up, confirming the expectation of a large amount of stopping and concomitant high baryon density in central Au nuclei collisions.

Figure 8 shows the m_t spectra for deuterons at $y=1.3$ for centralities ranging from the peripheral to the central. The spectra again are scaled up by a factor of 2 successively. It is clear that the spectrum in the central reactions is much flatter than that in the peripheral collisions. The straight lines are an attempt to fit the spectra with a single exponential. As discussed before, in general particle spectra deviate from a single exponential parameterization in central Au+Au reactions, so the fit in the figure is intended to be qualitative to discern any systematic trend of the spectrum shape for different centralities and/or reactions. This systematic comparison is summarized in Figure 9, where the inverse slope parameters for pions, protons, and deuterons are plotted for a combination of reactions at various centralities. The horizontal axis is the number of participants estimated from the centrality cut of the reactions. The solid points are from Au+Au reactions at 11.6 A-GeV/c, the open squares are data from p+Au reactions at 14.6 GeV/c, and the open diamond is from central Si+Au reaction at 14.6 A-GeV/c. For pions, there is little change of the inverse slope parameter from the p+Au reactions to that of the central Au+Au reactions. The inverse slope parameter increases for protons as the number of participants in the reactions increases, and the increase is most pronounced for deuterons. This is consistent with the picture that radial expansion exists after the high density stage is reached. In this picture, qualitatively speaking the larger the mass of a particle, the larger the transverse momentum it gains from the radial expansion - hence higher inverse slope parameter in its spectrum [11,12].

In the high baryon density environment, the final yield of the anti-proton is sensitive to many factors, both in its production and in its annihilation. The interesting question is whether the high baryon density environment would modify the free-space mechanism of production and annihilation in the absence of the high density. Considerable effort has been put in to the experimental measurement of the anti-protons yield, and now results are available in a large kinematic coverage. E866 is the experiment which covers the central rapidity for anti-proton with a reasonable

range in $m_t - m_0$. Figure 10 shows the anti-proton spectra around the central rapidity for three centrality ranges. The solid points are from E866 experiment, the open points from E878, and the cross from E864. The yields from E866 increase slowly as more central reaction is selected. As far as the shape is concerned, it is exponential for the peripheral reactions, and the low m_t end of the spectrum starts to bend down, like protons, for more central reactions. In comparison with models such as ARC [13], a shielding has to be introduced to reduce the annihilation in order to reproduce the final yield [14]. Unfortunately, discrepancy exists among the experimental data, and as an example Figure 10 summarizes the situation. Since data from E878 were taken in 1993 run where the beam momentum was 10.7 A·GeV/c, compared to a beam momentum of 11.6 A·GeV/c for the other two experiments, a scale up factor of 1.4 was introduced to facilitate a direct comparison. The factor 1.4 comes from an interpolation of anti-proton production in p-p reactions. In peripheral reactions, data from E878 is consistent with that of E866, and it gradually becomes somewhat lower in central reactions. One possible explanation for this could be that the centrality device in E878 is not effectively discriminating peripheral collisions from its central events, lowering its anti-proton yields in central collisions as a result. On the other hand, data from E864 seems high compared with that of E866 in the central collisions, but not in contradiction. The contradiction shows up when data from E864 and E878 are brought together for comparison, and there is about a factor of 4 difference between these two measurements. It was pointed out that the difference could be due to the anti-lambda contribution to E864, which accepts essentially all the anti-protons from the decay of anti-lambda while E878 takes none. Based on this assumption, one could estimate the yield of anti-lambda in the reactions, and the anti-lambda to anti-proton ratio was concluded to be $\bar{\Lambda}/\bar{p} = 5.9 \pm 2.5$ [15] at midrapidity near $p_t = 0$. This is a very large ratio, and it is worth to bear in mind that K^- yield from E864 is also somewhat high in comparison with that of E866.

III. SUMMARY

In summary, many new results have become available in Au+Au reactions at AGS energies. From the proton rapidity distribution it is concluded that a state of high baryon density has been achieved in central Au+Au reactions. A systematic comparison of inverse slope parameters for different particle species points out that radial expansion exists when the high density matter starts to disintegrate. More systematic effort on the anti-proton analysis is needed in order to resolve the current discrepancy among results from different experiments.

IV. ACKNOWLEDGMENT

This work was supported by the U.S. Department of Energy under contracts with BNL (DE-AC02-76CH00016). The author likes to thank Dr. S. Kahana for the invitation to participate in the workshop. It is the author's pleasure to thank the E802 collaboration for making excellent progresses in data analysis. It is also an appropriate opportunity for the author to thank people in BNL-HIRG group, especially Drs. C. Chasman and F. Videbaek, for help in many ways. At last the author likes to acknowledge Dr. T. Hemmick and Mr. T. Piazza for providing postscript files of E877 results.

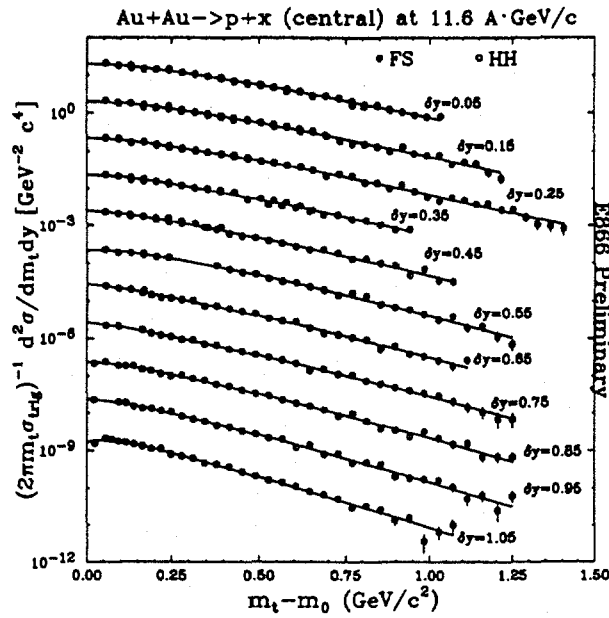


FIG. 1. E866 measured invariant cross-section divided by the trigger cross section for identified protons in different rapidity intervals as a function of transverse kinetic energy $m_t - m_0$. The bin width of the rapidity interval is 0.1, and δy is the distance of the measured rapidity of the spectra from the central rapidity $y_{nn} = 1.6$. The spectra are scaled down by a factor of 10 successively.

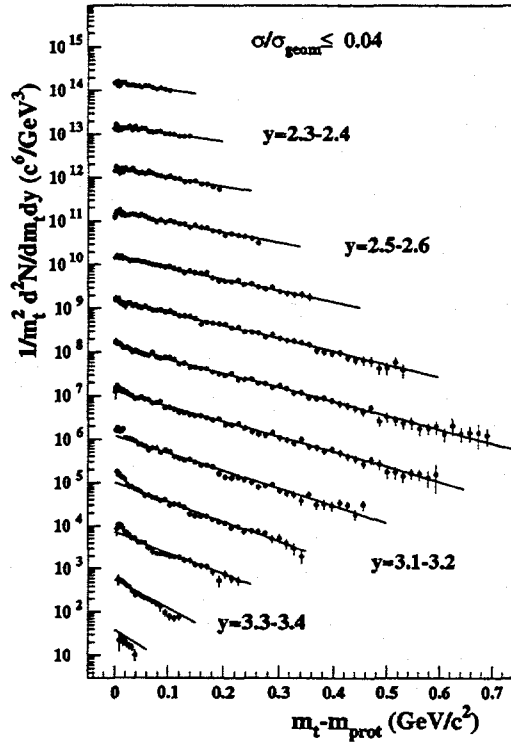


FIG. 2. The preliminary results of E877 measured spectra for identified protons in different rapidity intervals as a function of transverse kinetic energy $m_t - m_0$. The bin width of the rapidity interval is 0.1. The spectra are scaled up by a factor of 10 successively.

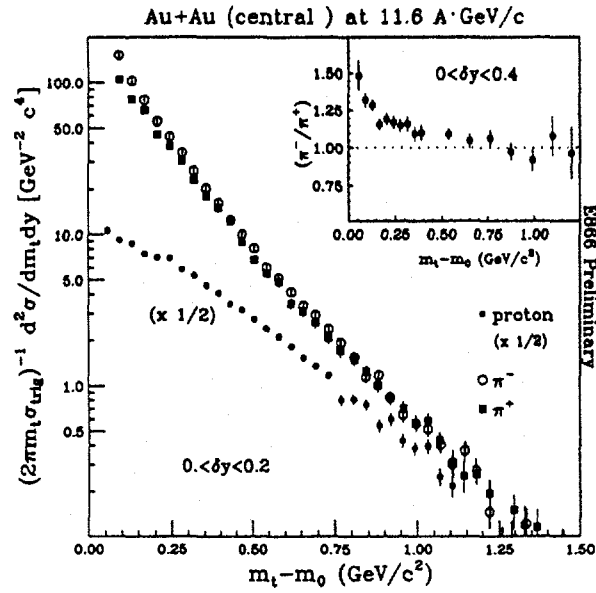


FIG. 3. E866 measured invariant cross-section divided by the trigger cross section for identified pions and protons in the rapidity interval $0 < \delta y < 0.2$ as a function of transverse kinetic energy $m_t - m_0$. The spectra for protons, plotted as solid round points, is scaled down by a factor of 2. The open circles in the figure are the spectra for π^- , and the solid squares are that for π^+ . The insert shows the ratio of π^-/π^+ as a function of $m_t - m_0$ in a larger rapidity interval, $0 < \delta y < 0.4$.

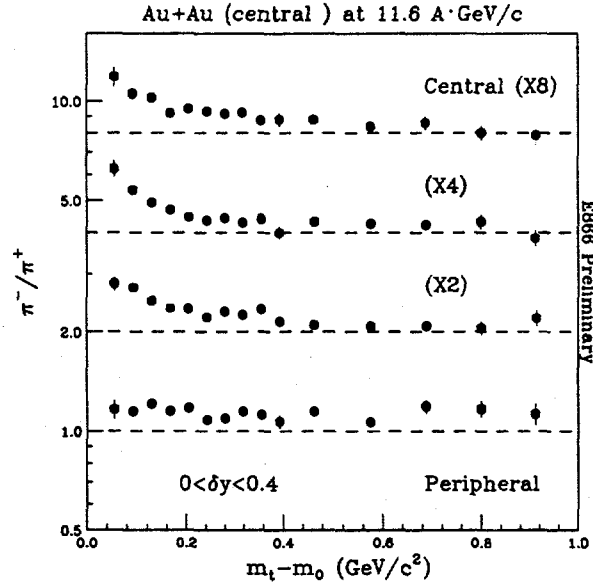


FIG. 4. The centrality dependence of the ratio, π^-/π^+ , for Au+Au reactions at 11.6 A·GeV/c. The ratio is scaled up successively by a factor of 2 from the peripheral to the central. The data is from E866.

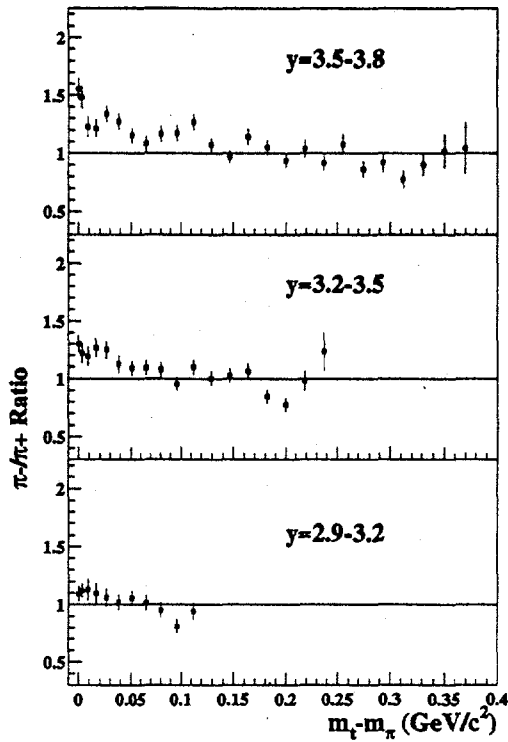


FIG. 5. The π^-/π^+ ratio as a function of $m_t - m_0$ in different rapidity bins. The figure is a preliminary result from E877.

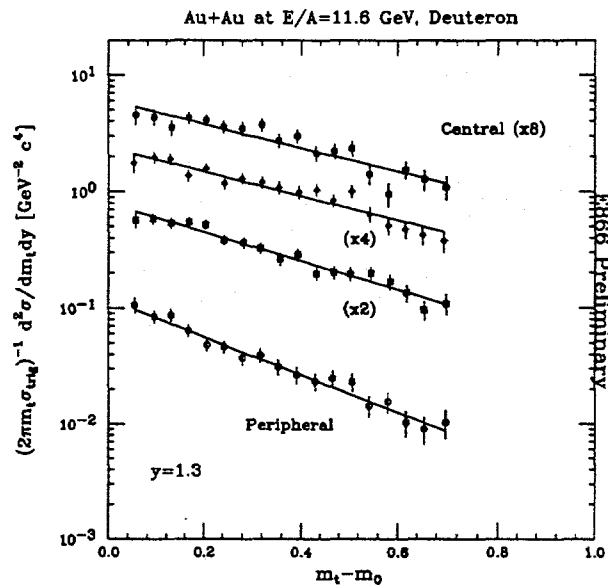


FIG. 6. Centrality dependence of the deuteron m_t spectra at rapidity $y=1.3$. The spectra are scaled up by a factor of 2 successively as more central events are selected.

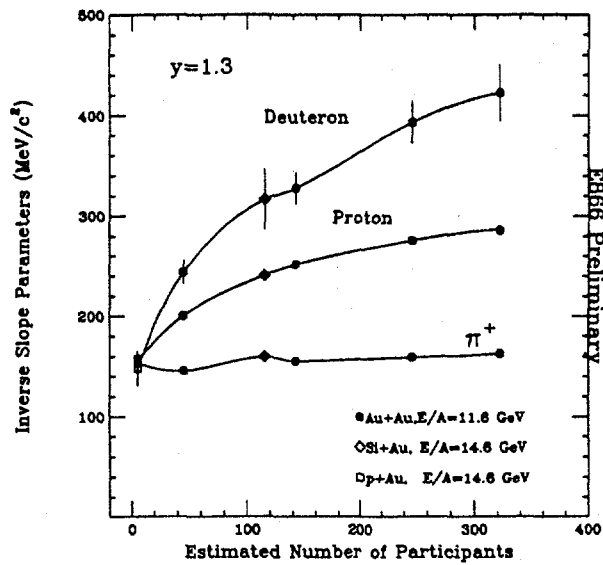


FIG. 7. Inverse slope parameters as a function of the estimated number of participants in the reactions for pions, protons, and deuterons. The data included in the figure are from p+Au reactions at 14.6 GeV/c, Si+Au reactions at 14.6 A-GeV/c, and Au+Au reactions at 11.6 A-GeV/c.

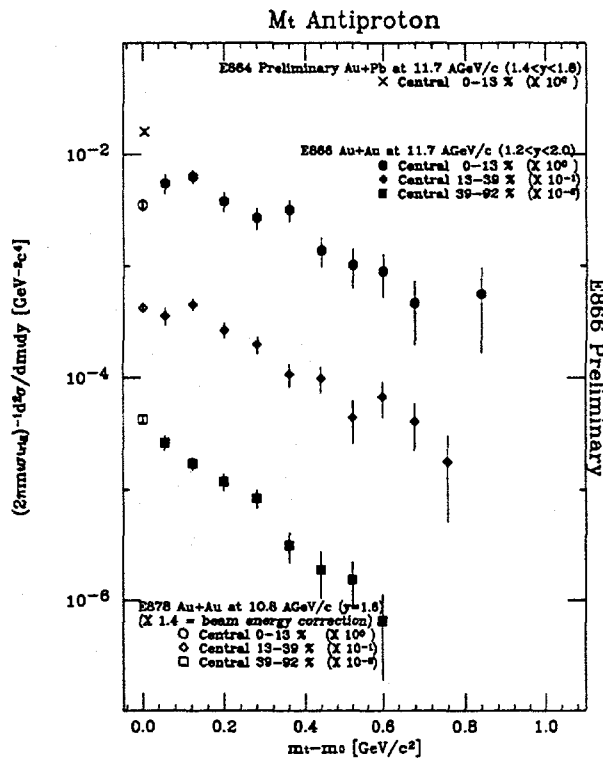


FIG. 8. Comparison of anti-proton yields among E866, E878, and E864 for three selected centralities. The solid points are from E866, the open points from E878, and the cross from E864. In central collision, the discrepancy between E864 and E878 is obvious (see text for more details).

-
- [1] E-802 Collaboration, T. Abbott et al., Phys. Lett. B 197, 285 (1987).
 - [2] T. Piazza, Private communication.
 - [3] E-802 Collaboration, T. Abbott et al., Phys. Rev. D 45, 3906 (1992).
 - [4] E-802 Collaboration, T. Abbott et al., Phys. Rev. Lett. 64, 847 (1990).
 - [5] E-802 Collaboration, T. Abbott et al., Phys. Rev. C 50, 1024 (1994).
 - [6] R. Brockmann et al. Phys. Rev. Lett. 53, 2012 (1984).
 - [7] R. Stock, Phys. Rep. 135, 259 (1986).
 - [8] J. P. Sullivan et al. Phys Rev C 24 1499 (1981).
 - [9] H. Böggild et al. Phys. Lett. B 372 339 (1996).
 - [10] M. Gyulassy and S.K. Kauffmann, Nucl. Phys. A 362 503 (1981).
 - [11] P.J. Siemens and J. O. Rasmussen, Phys. Rev. Lett. 42, 880 (1979).
 - [12] R. Mattiello et al., Phys. Rev. Lett. 74, 2180 (1994).
 - [13] S. Kahana et al. Proceedings of HIPAGS '93, page 26, edited by G. Stephans, S. Steadman, and W. Kehoe (MITLNS-2158).
 - [14] B.S. Kumar et al. Nucl. Phys. A566 439c-442c (1994).
 - [15] J.G. Lajoie et al. Proceedings of HIPAGS'96, edited by S. Bennett and C. Pruneau (to be published).